Single-Event Leakage Current and Single-Event Burnout in High-Voltage GaN and SiC PiN Diodes: A Comparative Analysis

Grant M. Mayberry, *Graduate Student Member*, *IEEE*, Xianduo Zhao, Herbert Gingold, Patrick Maloney, Sajal Islam, *Member, IEEE*, Arijit Sengupta, *Member, IEEE*, Xiao Shen, Aditha S. Senarath, Bingyu Zhang, Dylan Nguyen, Shannon Hankinson, Benjamin Bolton, Owen Meilander, Luke Yates, Robert J. Kaplar, *Senior Member, IEEE*, Aaron Franklin, *Fellow, IEEE*, Steven L. Kosier, *Senior Member, IEEE*, En Xia Zhang, *Senior Member, IEEE*, Daniel M. Fleetwood, *Life Fellow, IEEE*, Tania Roy, *Member, IEEE*, Mona A. Ebrish, *Senior Member, IEEE*, Sokrates T. Pantelides, *Fellow, IEEE*, Ronald D. Schrimpf, *Life Fellow, IEEE*

***Abstract*—Recent developments in GaN power devices challenge the long-standing success of SiC due to GaN's more advantageous material properties. Models, such as the critical-energy storage and release model, have been developed to explain and predict observed Single-Event Leakage Current (SELC) and Single-Event Burnout (SEB) thresholds for SiC technologies. However, GaN devices have not been tested and compared in the same high-voltage range as SiC. In this work, high-voltage GaN and SiC vertical PiN diodes were tested for SELC/SEB at similar voltages for a wide LET range. The experimental comparison shows a lower SELC/SEB tolerance in GaN, both in terms of raw voltage and critical stored energy (U_{SEE}). Defect measurements in GaN devices after SELC show a strong $E_C - 0.6\ eV$ trap presence that is attributed to SELC-generated N interstitials. The lower SEE tolerance of GaN is attributed to lower defect-multiplication activation energies, marking a limitation in GaN as a material, not simply an underdeveloped technology.**

***Index Terms*—Single-Event Effects (SEEs), Single-Event Leakage Current (SELC), Single-Event Burnout (SEB), Power devices, P-i-N Diodes, Deep-Level Transient Spectroscopy (DLTS), defects, junction energy storage, critical-energy storage and release model**

I. Introduction

HIGH-VOLTAGE power electronics find their way into the electric power grid and many modern technologies, such as avionics, satellites, defense systems, spacecraft, and electric vehicles [1,2]. With higher voltages comes higher efficiencies for power transmission [3]. As voltage requirements increase, the ability of silicon to form these critical components, with only a breakdown electric field of ~3×10^5 V/cm, diminishes, particularly for size- and weight-sensitive applications such as aviation and space.

Silicon carbide (SiC) has long been commercially successful as a wide-bandgap (WBG) material for power electronics, owing to its much higher breakdown electric field of ~3×10^6 V/cm, which enables a Baliga figure-of-merit approximately 10^3 times higher for power device applications [1,4]. However, with this high electric field comes the radiation problem of catastrophic single-event effects (SEEs). A single particle can strike the device at high reverse bias and cause reverse-

This work was supported in part by the US Air Force Center of Excellence in Radiation Effects via Grant No. FA9550-22-1-0012, the US DoD Multidisciplinary University Research Initiative "ReDesign" program, National Aeronautics and Space Administration (NASA) Silicon Carbide for High Voltage in Radiation Environments (SHiRE) under contract number 80NSSC26K0163, and Defense Common Parts Testing in Radiation (DECPTR) Project under contract number 2109.

Grant M. Mayberry and Sokrates T. Pantelides are with the Department of Physics and Astronomy and with the Department of Electrical and Computer Engineering, Vanderbilt University, Nashville, TN 37235 USA (e-mail: grant.m.mayberry@vanderbilt.edu; pantelides@vanderbilt.edu).

Xianduo Zhao, Bingyu Zhang, Dylan Nguyen, Aaron Franklin, and Tania Roy are with the Department of Electrical and Computer Engineering, Duke University, Durham, NC 27708 USA (e-mail: jerry.zhao@duke.edu; bingyu.zhang@duke.edu; dylan.nguyen@duke.edu; aaron.franklin@duke.edu; tania.roy@duke.edu).

Herbert Gingold, Patrick Maloney, Shannon Hankinson, Benjamin Bolton, and En Xia Zhang are with the Department of Electrical and Computer Engineering, University of Central Florida, Orlando, FL 32816 USA (e-mail: he073578@ucf.edu; patrick.maloney2@ucf.edu; shannon.hankinson@ucf.edu; benjamin.bolton@ucf.edu; Enxia.Zhang@ucf.edu).

Sajal Islam is with the Center for Reliable & Trusted Electronics (IU CREATE), Indiana University, Bloomington, IN 47408, USA (e-mail: sajislam@iu.edu). He was formerly with the Interdisciplinary Materials Science Program, Vanderbilt University, Nashville, TN 37235, USA.

Arijit Sengupta is with the Deutsches Zentrum für Luft- und Raumfahrt e. V. (DLR) Institut für Elektrifizierte Luftfahrtantriebe, Lieberoser Str. 13A, 03046 Cottbus, Germany (e-mail: arijit.sengupta@Vanderbilt.Edu). He was formerly with the Department of Electrical and Computer Engineering, Vanderbilt University, Nashville, TN 37235, USA.

Aditha S. Senarath is with Global Foundries, Essex Junction, VT 05452, USA. He was formerly with the Interdisciplinary Materials Science Program, Vanderbilt University, Nashville, TN 37235, USA.

Owen Meilander is with the Interdisciplinary Materials Science Program, Vanderbilt University, Nashville, TN 37235 USA (e-mail: owen.meilander@Vanderbilt.Edu).

Xiao Shen is with the Department of Physics and Materials Science, University of Memphis, Memphis, TN 38152 USA (e-mail: xshen1@memphis.edu).

Luke Yates and Robert J. Kaplar are with the Semiconductor Material and Device Sciences Department, Sandia National Laboratories, Albuquerque, NM 87123 USA (e-mail: lyates@sandia.gov; rjkapla@sandia.gov).

Steven L. Kosier, Daniel M. Fleetwood, Mona A. Ebrish, and Ronald D. Schrimpf are with the Department of Electrical and Computer Engineering and/or the Institute for Space and Defense Electronics, Vanderbilt University, Nashville, TN 37235 USA (e-mail: steven.kosier@vanderbilt.edu; dan.fleetwood@vanderbilt.edu; mona.ebrish@Vanderbilt.Edu; ron.schrimpf@Vanderbilt.Edu).

bias leakage current to increase suddenly and permanently (Single-Event Leakage Current, SELC), or, at higher voltages, short the device altogether (Single-Event Burnout, SEB) [5]. These phenomena have been attributed in part to the energy stored in the capacitor-like structure of a power device [6]-[8], to be explained in detail later.

In recent years, gallium nitride (GaN) has gained attention for power devices [3], due to its slightly higher breakdown electric field and electron mobility compared to SiC [1]. This feature makes GaN well suited for power devices [9], but it may not translate to radiation hardness [10].

This work provides a direct comparison of multi-kV vertical GaN and SiC PiN diodes under heavy-ion irradiation. These data are evaluated using the critical-energy storage and release framework [6]-[8], demonstrating that the radiation hardness of vertical GaN devices in the multi-kV range is markedly lower than that of SiC. We then connect post-irradiation leakage behavior in GaN to measured defect signatures. We find that the defect measurements are consistent with a defect-multiplication picture [11,12], suggesting that GaN is less tolerant of SELC/SEB than SiC at a material level, rather than due to device manufacturing processes.

II. Experimental Methodology

For all devices, the incident ion ranges exceed epitaxial layer thicknesses, ensuring full traversal of the depletion region during irradiation. Junction energy storage was calculated using measured reverse-bias *C-V* characteristics and the metallurgical junction area, as described in Section III.

A. 3.2 kV GaN PiN Diodes

3.2 kV GaN PiN diodes were fabricated at Naval Research Labs on a single die. The die was then diced, packaged, and sent to Texas A&M University's (TAMU) Radiation Effects Facility for SEE testing. 15 MeV Ar and Pr were selected for their useful low (6.1 MeV·cm^2/mg) and high (44.1 MeV·cm^2/mg) LETs in GaN, respectively. An initial forward and reverse *I-V* sweep was done to ensure the devices worked properly. Then, with the beam on, the reverse voltage was ramped up from 0 V to 3 kV, at a rate chosen to ensure a total fluence of ~10^7 cm^{-2} ions by the end of the sweep, enough to observe catastrophic SEEs while limiting cumulative damage. After marking the onset voltages of SELC/SEB, the voltage was taken 50 V below that onset voltage for the next device to pinpoint the threshold of SELC/SEB. This process of lowering voltage was continued until no SELC/SEB occurred. The minimum reverse-bias voltage at which SELC/SEB was observed was defined as the threshold voltage for that SEE and used in subsequent junction energy storage calculations. Identical testing on 3.3 kV SiC PiN diodes using the same experimental setup and incident ions during the same beam session is reported elsewhere [13].

B. 6 kV GaN PiN Diodes

6 kV GaN PiN diodes were fabricated at Sandia National Laboratories [9,14]. There was greater variation in the size and shape of the edge termination in these devices. Most notably, there were a set of devices with an anode radius of 142 µm (denoted here as "small"), and a set of devices with an anode radius of 563 µm (denoted here as "large"). Before any bonding or radiation testing, forward and reverse *I-V* (–1000 V to +5 V) and *C-V* (0 to –500 V) measurements were taken from 10 K to 350 K to ensure predictable device behavior. This was done to establish a strong baseline of operation for these devices, as they would be analyzed more extensively than their 3.2 kV counterparts. Devices were sent to the Lawrence Berkeley National Laboratory (LBNL) 88-inch Cyclotron and tested using the same methods as the 3.2 kV devices. However, the ions used were 20 MeV Cu (11.6 MeV·cm^2/mg) and 20 MeV Xe (37.2 MeV·cm^2/mg). One 8 kV SiC PiN diode from GeneSiC was tested with 20 MeV Cu (15.2 MeV·cm^2/mg) to ensure accurate correspondence with previous SiC data. After beam testing, six GaN devices were left in a leakage (degraded) state, and one burned out. Forward and reverse *I-V* and *C-V* curves were taken to aid analysis.

C. Defect Measurements

Current-based Deep-Level Transient Spectroscopy (I-DLTS) [15] measurements were performed on two of the 6 kV GaN devices that had exhibited SELC. I-DLTS measurements were employed specifically because the devices were very leaky, and standard DLTS [16] measurements failed. I-DLTS works by abruptly biasing the device to a high reverse bias from 0 V. The current transient that results from the emission of trapped charges is measured. I-DLTS measurements were analyzed in the following way: The current transient $I(t)$ from a single emitting trap level at a concentration N_T, with an emission rate e_n, for a depletion width change of x_d, is given by

$$I(t) = -\tfrac{1}{2} qAx_d N_T e_n \exp(-e_n t)\ . \qquad (1)$$

If the transient of current is given by (1) and the response is dominated by a single trap level, with some spread, then the total current can be fit to

$$I(t) = I_\infty + \alpha \exp\left(-\left(\tfrac{t}{\tau}\right)^{\beta}\right), \qquad (2)$$

where I_∞ is a free parameter corresponding to the DC current response of the device, α is a free parameter corresponding to the pre-exponential factor in (1), τ is a free parameter corresponding to the time constant of the trap, and β is a free parameter corresponding to the width or spread of the trap energy levels [15]. Based on the above equations, N_T can be found using

$$N_T = -\frac{2\alpha\tau}{qAx_d}\,. \qquad (3)$$

At multiple temperatures, an Arrhenius plot of the time constants can be constructed in accordance with

$$\tau^{-1} = CT^2 e^{-E_a/kT}\ , \qquad (4)$$

where T is the temperature of the measurement, k is the Boltzmann constant, C is a constant, and E_a is the activation energy associated with the trap(s) leading to the temperature dependence of the observed response. The slope of a plot of $\ln(\tau T^2)$ vs $1/kT$ gives E_a [15], [16].

III. Results

A. Heavy-Ion Testing Results

The combined results of the TAMU and LBNL experiments for all devices are shown in Fig. 1, which includes data from [13,17] as well. On the *x*-axis is the LET of the ion in a particular test, and on the *y*-axis is the voltage at which the SEE was observed. The data from [13] are from the same ion beam and experimental setup as the 3.2 kV GaN PiN diodes. Since the devices have different levels of doping, this plot does not allow us to unambiguously determine which material is more resistant to SELC and SEB. It is for this reason that widely available voltage vs. LET data are not useful for material comparison.

A recently developed critical-energy storage and release model [6]-[8], which posits that the junction energy stored in the depletion region determines the voltage thresholds for SELC and SEB, enables the plots of Fig. 2, with energy stored in the depletion region on the *y*-axis instead of voltage. The model successfully explains the SEB voltage thresholds of SiC power devices with various epitaxial doping levels, so it is applied here in GaN as well to allow a direct material comparison.

During an ion strike, the energy stored within the capacitor-like structure (U_{SEE}) is assumed to provide the necessary energy to cause material degradation or device failure. In general, U_{SEE} is given by

$$U_{SEE} \equiv \frac{1}{A}\int_{\Omega} V\, dQ = \frac{1}{A}\int_{0}^{V_{SEE}} V\, C(V)\, dV, \qquad (5)$$

where A is the area of the metallurgical junction, Ω is the depletion region, V_{SEE} is the applied voltage when the SEE is observed, and $C(V)$ is the capacitance of the junction at the given voltage. For the one-dimensional case with a uniformly and lightly *n*-doped epitaxial layer, (5) gives

$$U_{SEE} = \frac{1}{3}\sqrt{2q\varepsilon_0\varepsilon N_D}\cdot {V_{SEE}}^{3/2}\,, \qquad (6)$$

where q is the elementary charge, ε_0 is the permittivity of free space, ε is the material's relative permittivity, and N_D is the epitaxial doping, as shown in [8].

In this work, U_{SEE} was calculated using measured reverse-bias capacitance–voltage characteristics according to (5), which implicitly accounts for device geometry, depletion width evolution, and non-uniform doping profiles without requiring explicit assumptions regarding epitaxial thickness or electric-field distribution. Nevertheless, representative doping concentrations for all devices is shown in Table 1. The striking ion produces a conducting plasma of electron-hole pairs, which shorts the depletion region and rapidly drains the stored energy. For higher LET, the stored energy (U_{SEE}) is drained more rapidly, and the underlying material experiences greater damage, so a combination of high U_{SEE} and high LET is necessary.

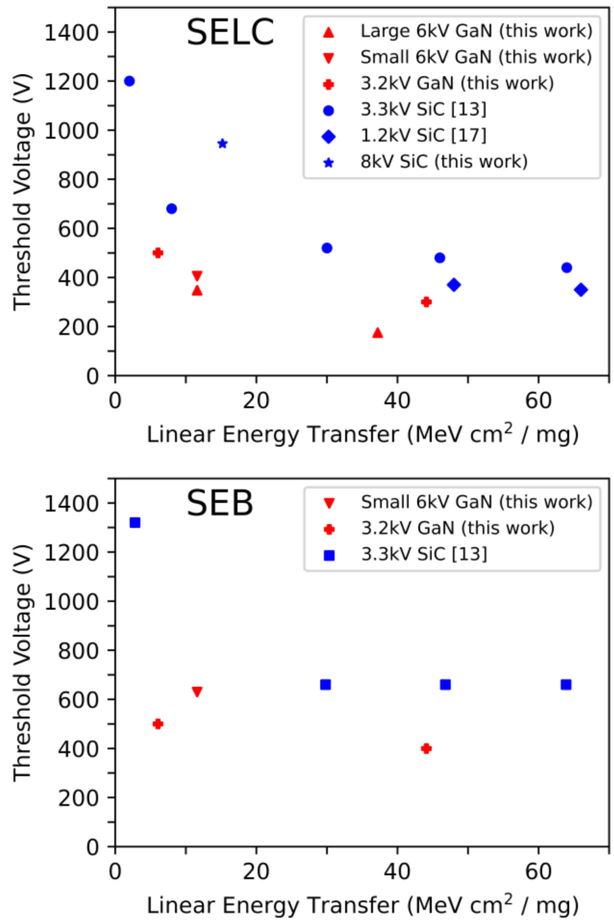

Fig. 1. Threshold voltage vs. LET data for SiC (blue) and GaN (red) PiN diodes, showing SELC (top) and SEB (bottom). The experimental data from [13] are obtained at the same ion beam facility at TAMU using the same experimental setup. More than two large 6 kV GaN diodes experienced SELC, but the lowest numbers are reported. Because of the different device doping, these figures do not allow for clear and umanbiguous material comparison. A model such as a critical-energy storage and release model [6]-[8] must be used to remove this doping dependence. The results are shown in Fig. 2.

Table I
Doping Levels for All Devices

Device	Doping (cm^{-3})
1.2 kV SiC	8×10^{15}
3.2 kV GaN	5×10^{15}
3.3 kV SiC	3×10^{15}
6 kV GaN	7×10^{14}
8 kV SiC	9×10^{14}

Represetative doping concentrations for all devices shown in Figs. 1 and 2.

There is a slight advantage shown in the small 6 kV GaN diodes compared to the large 6 kV GaN diodes. Previous studies have shown that anode design can have an impact on electric field management [18,19], which would have an effect on the pre-strike stored energy that is not captured by the ideal one-dimensional perspective of (5) and (6). The large 6 kV GaN devices also became so leaky due to SELC events that determining SEB thresholds became impractical. Previous experiments have shown that different edge terminations in GaN PiN diodes leading to different electric field management can translate to a

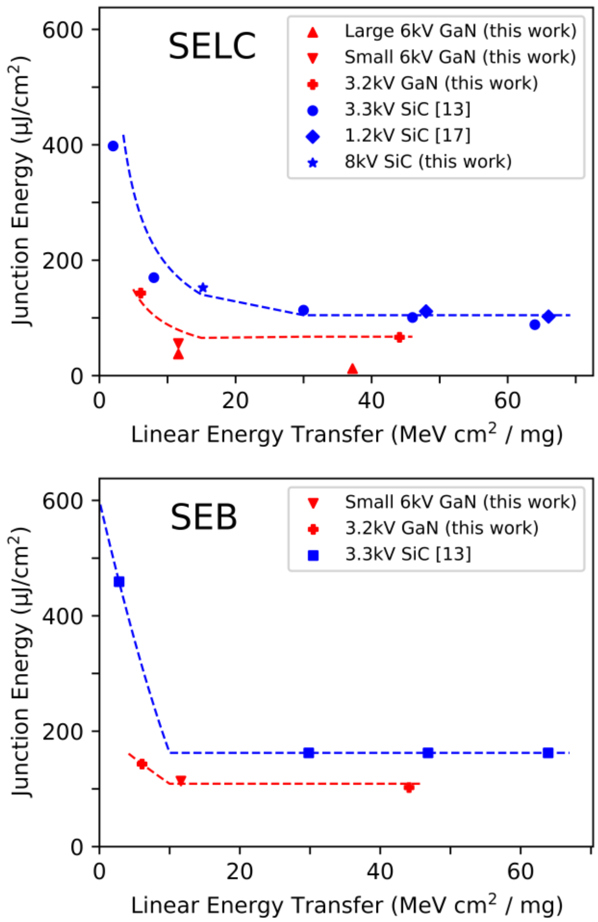

Fig. 2. Threshold stored junction energy vs. LET data for SiC (blue) and GaN (red) PiN diodes, showing SELC (top) and SEB (bottom). The critical-energy storage and release model [6]-[8] was used to compare devices with different doping and voltage ratings. A markedly lower performance of GaN devices is observed across various doping concentrations and LETs and for multiple device structures, suggesting that GaN has less advantageous material properties. The experimental data from [13] are obtained at the same ion beam facility at TAMU using the same experimental setup. More than two large 6 kV GaN diodes experienced SELC, but the lowest numbers are reported; however, all U_{SELC} values are within 5 μJ/cm^2 of the reported value, so there is little variation in those results. The large 6 kV GaN data are not included in the SELC fit because of its lower radiation tolerance than the small 6 kV GaN due to its disadvantageous structure.

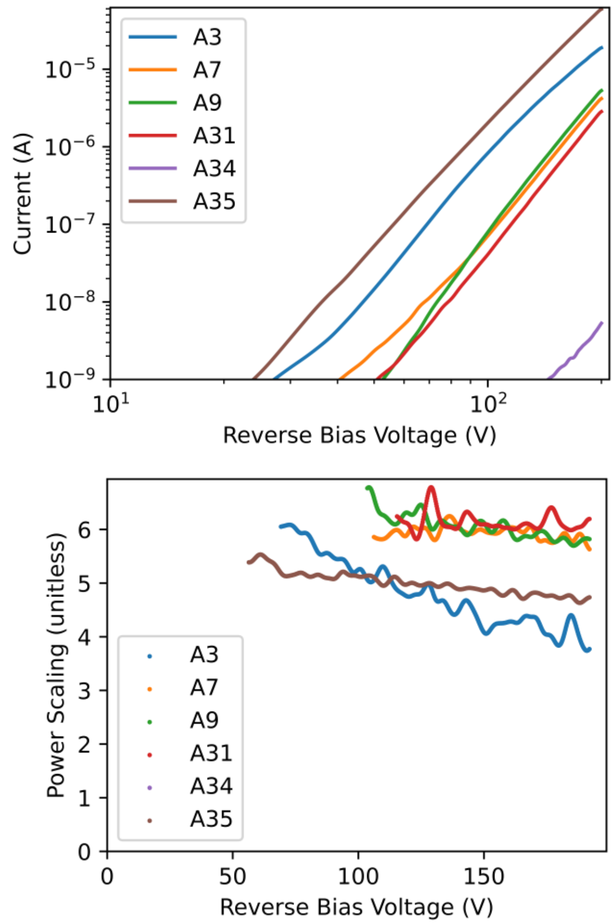

Fig. 3. Reverse I-V characteristics for devices in the LBNL experiment. The raw data are shown on the top and the slope of the log-log plot is shown on the bottom. The high power scaling that scales upward with decreasing leakage magnitude is consistent with the leakage being hopping limited.

more or less robust response to Cf-252 fission fragments and other low-range ions [20,21]. The less robust Junction Termination Extension was employed on all the 6 kV GaN devices, explaining the increased robustness of the 3.2 kV GaN devices by comparison. If these structural differences lead to regions within the devices where more energy is stored across the junction area, then those regions would be more susceptible to SELC/SEB failure.

However, for these multiple device structures and doping, the high-voltage GaN diodes were statistically less robust to both SEB and SELC compared to SiC, suggesting that material properties are responsible for the difference. The lower robustness of GaN holds for all the multiple edge terminations and sizes tested in 6 kV GaN diodes. No combination of doping, edge termination, or anode radius was able to overcome the robustness of SiC at any LET range. The fact that the GaN data follow the same general shape as the SiC data suggests a common mechanism, so extensive previous insights into SELC/SEB in SiC may prove useful in the GaN material system.

B. Post-Irradiation Measurements

Post-irradiation reverse *I-V* curves for some of the devices irradiated in the LBNL experiment are shown in Fig. 3. All these devices are 6 kV vertical GaN PiN diodes that only experienced SELC. On the right is the slope of the log-log plot of the reverse *I-V* characteristics on the left. The devices with a higher leakage current have a lower power-scaling factor (the slope of the log-log plot) than the less leaky devices. Such behavior is consistent with hopping conduction, since the probability of trap-to-trap hopping increases dramatically with increasing electric field for systems with fewer available hopping sites [22]-[25]. Thus, rate-limiting factor in the leakage of the devices is likely hopping conduction, even for such a thick epitaxial layer.

I-DLTS measurements were performed on two 6 kV GaN diodes, denoted A3 and A7, each exhibiting a different post-SELC leakage-current level. The results of these I-DLTS measurements are shown in Fig. 4. Two pristine devices, denoted A11 and A22, were also measured, but showed no meaningful result for the I-DLTS measurement. The results of Fig. 4 demonstrate that the concentration of the identified trap scales with leakage current, strongly suggesting that the $E_C - 0.6\ eV$ trap is associated with post-SELC leakage current paths in vertical GaN power devices.

IV. Discussion

Iron has long been known as an impurity in GaN electronic devices [26]-[31]. It is intentionally introduced in GaN/AlGaN HEMTs to create an insulating blocking layer. After many years of efforts to identify the prominent Fe-related deep acceptor level at ~0.6 eV below the conduction-band edge, it was recently established that it is simply substitutional Fe at Ga sites (Fe_{Ga}) [31]. The presence of Fe impurities in GaN vertical power devices has been examined in detail by many investigators. The key finding is that, depending on the process used for fabrication, Fe is present at levels up to ~10^{17} cm^{-3} and decays below the detection limit within a few microns from the substrate [32].

Our devices are grown by a process that includes layers intended to isolate contaminants from the active device regions. The devices have consistently demonstrated uniform net drift-region doping, signaling that the concentration of Fe_{Ga} centers that are not passivated by hydrogen is well below the n-type doping level in the 50-µm drift region. In control power devices that were irradiated without bias simultaneously with the devices under bias, we found that the 0.6-eV level concentration is below the doping concentration. The fact that the 0.6-eV level is observed in a range from 10^{15} to 10^{18} cm^{-3} by I-DLTS (Fig. 4d) suggests that Fe_{Ga} may contribute to, but is not the dominant component of, the I-DLTS signal from the SELC-generated 0.6-eV level.

Given the above, the results shown in Fig. 2 demonstrate that GaN is less radiation tolerant than SiC for SEEs in these high-voltage vertical power devices. This finding is true for devices of different sizes, edge-terminations, doping, and breakdown voltages. The observed difference in SEE robustness cannot be attributed solely to device or processing variability, as the trend persists across multiple designs and fabrication sources.

A possible defect multiplication mechanism within an energetic ion track in compound semiconductors was recently discovered by first-principles calculations for GaN by a subset of the present authors [11]. In subsequent work, further calculations found that anion vacancy multiplication, enabled by the high applied voltage, is the driving mechanism behind SELC, with SEB being a runaway SELC [12]. The calculated energy for this process is lower in GaN than in SiC, suggesting that SELC and SEB should occur at a lower U_{SEE} in GaN than in SiC, which is exactly what is seen experimentally in Fig. 2. Furthermore, the fact that the observed leakage currents in the tested devices appear to be hopping-limited is consistent with occasional hopping between anion-vacancy-chain segments.

Returning to the 0.6-eV defect level, given the above description of the SELC process, we examine intrinsic point defects that can possibly be generated by the defect multiplication

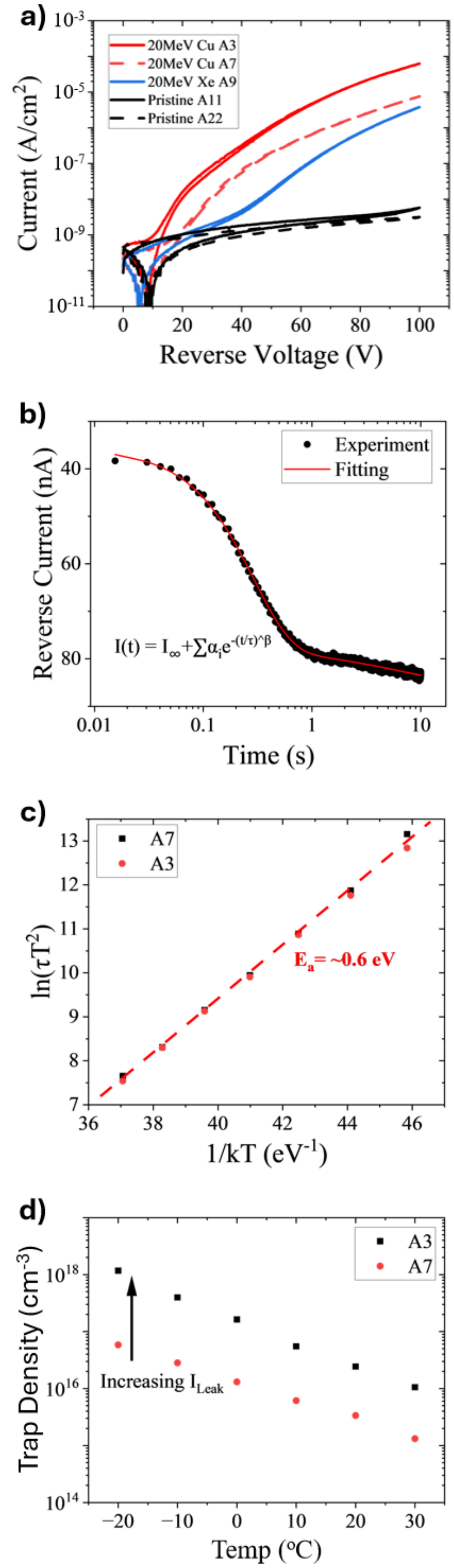

Fig. 4. I-DLTS results for 6 kV GaN devices after experiencing SELC. a) Reverse I-V curves of the devices in question compared to pristine devices. b) An example of time constant extraction from fitting (2) to current transient data taken at 10 °C. c) Trap level extraction from an Arrhenius plot identifying a trap at $E_C - 0.6\ eV$ in accordance with (4). d) Trap density given by (3).

process. Vacancies, interstitials, antisite defects and their complexes are the only candidates. Of these, N vacancies and V_{Ga}-V_N divacancies have energy levels that are smaller than 0.6 eV and are therefore too fast to be detectable by room-temperature I-DLTS and are masked by the 0.6-eV defect level. However, their energy levels have been calculated by theory and detected by low-frequency noise at lower temperatures [10], [26], [33]-[38]. A table of energy levels calculated by different authors for intrinsic defects in GaN shows that the only viable candidate is interstitial N, N_i [38]. The latest calculations by Hauck et al. [38] found this defect to have a (0/–) deep acceptor level at ~0.6 eV. Averaging this level with three prior calculations listed in the table gives 0.7±0.2 eV.

The defect-multiplication process generates large numbers of both N vacancies and N interstitials. N vacancies have large migration energies (>2.5 eV) because of the second-neighbor jumps [39]. N interstitials, on the other hand, have relatively smaller migration energies and can escape from the ion track in the Joule-heat drop-off region outside the track. As the material cools after an SELC event, N_i's in the negatively charged state remain stable as their migration energy is large (1.6 eV), and they only become mobile at temperatures around 200 °C [39].

In conclusion, the defect-multiplication mechanism provides an explanation for both the SELC events and the appearance of negatively charge N interstitials that are detected by the DLTS measurements.

V. Conclusions

In conclusion, multi-kV vertical GaN PiN diodes exhibit higher susceptibility to catastrophic SEEs than comparable SiC devices when evaluated using the critical-energy storage and release model. SELC events in these GaN diodes are associated with the formation of hopping-limited leakage paths driven by radiation-induced, high-reverse-bias enabled defect-multiplication. Results of both reverse bias *I-V* and I-DLTS measurements are consistent with first-principles calculations which indicate that the energy barrier for defect-multiplication in GaN is lower relative to SiC.

The predicted defect species and behavior is also consistent with defect measurement results. These results demonstrate that defect energetics, rather than breakdown field alone, fundamentally limit the radiation hardness of next-generation wide-bandgap power devices. GaN may still hold an advantage in high-speed switching applications, and for voltages of about 600 V or less, where commercial SiC power devices are not available. However, the materials' radiation hardness, based on experimental results that are consistent with previous theoretical literature, suggest that SiC is preferable over GaN for vertical multi-kV power devices in radiation environments.

Acknowledgment

The authors thank Sandia National Laboratories for providing the GaN and SiC devices used in this study. The authors also thank Brendon Gunning for growth of the vertical GaN material and Swarnim Neema of Vanderbilt University for early discussions regarding the 6 kV GaN devices.

References

[1] J. Y. Tsao et al., "Ultrawide-bandgap semiconductors: Research opportunities and challenges," *Adv. Elect. Mater.*, vol. 4, Dec 2017, Art. no. 1600501, doi: https://doi.org/10.1002/aelm.201600501.

[2] S. Pearton, A. Haque, A. Khachatrian, A. Ildefonso, L. Chernyak, and F. Ren, "Review—Opportunities in single event effects in radiation exposed SiC and GaN power electronics," *ECS J. Solid State Sci. Technol.*, vol. 10, Jun 2021, Art. no. 075004, doi: 10.1149/2162-8777/ac12b8.

[3] K. Woo et al., "From wide to ultrawide-bandgap semiconductors for high power and high frequency electronic devices," *J. Phys. Mater.*, vol. 7, Mar 2024, Art. no. 022003, doi: 10.1088/2515-7639/ad218b.

[4] B. J. Baliga, "Semiconductors for high-voltage, vertical channel field-effect transistors," *J. Appl. Phys.*, vol. 53, no. 4, pp. 1759-1764, Mar 1982, doi: 10.1063/1.331646.

[5] S. J. Pearton et al., "Review—Radiation damage in wide and ultra-wide bandgap semiconductors," *ECS J. Solid State Sci. Technol.*, vol. 10, Apr 2021, Art. no. 055008, doi: 10.1149/2162-8777/abfc23.

[6] S. L. Kosier et al., "Physical model for SiC power device heavy-ion burnout based on pre-strike depletion capacitance energy storage," *IEEE Trans. Nucl. Sci.*, vol. 72, no. 4, pp. 1418-1424, Apr 2025, doi: 10.1109/TNS.2025.3546892.

[7] A. Sengupta et al., "Physical models for epitaxial doping dependence of single-event leakage current in SiC power devices," *IEEE Trans. Nucl. Sci.*, vol. 73, no. 4, pp. 1189-1195, Nov 2025, doi: 10.1109/TNS.2025.3630040.

[8] S. L. Kosier et al., "Ideal specific on-resistance versus single-event burnout and leakage voltage thresholds in vertical SiC power devices," *IEEE Trans. Device Mat. Rel..*, vol. 26, no. 2, pp. 648-651, Jun 2026, doi: 10.1109/TDMR.2026.3689763.

[9] R. J. Kaplar et al., "Development of high-voltage vertical GaN PN diodes," *2020 IEEE International Electron Devices Meeting (IEDM)*, San Francisco, CA, USA, 2020, pp. 5.1.1-5.1.4, doi: 10.1109/IEDM13553.2020.9372079.

[10] D. M. Fleetwood, E. X. Zhang, R. D. Schrimpf, and S. T. Pantelides, "Radiation effects in AlGaN/GaN HEMTs," *IEEE Trans. Nucl. Sci.*, vol. 69, no. 5, pp. 1105-1119, May 2022, doi: 10.1109/TNS.2022.3147143.

[11] A. O'Hara, R. D. Schrimpf, D. M. Fleetwood, and S. T. Pantelides, "Defect dynamics in the presence of excess energetic carriers and high electric fields in wide-gap semiconductors," *J. Appl. Phys.*, vol. 135, no. 19, May 2024, Art. no. 195701, doi: 10.1063/5.0203047.

[12] G. M. Mayberry, X. Shen, D.-L. Bao, D. Negash, D. R. Ball, D. M. Fleetwood, R. D. Schrimpf, and S. T. Pantelides, "First-principles radiation-robustness ranking of wide-bandgap semiconductors," (*to be published*)

[13] A. Sengupta et al., "LET and voltage dependence of single-event burnout and single-event leakage current in high-voltage SiC power devices," *IEEE Trans. Nucl. Sci.*, vol. 71, no. 4, pp. 809-815, Jan 2024, doi: 10.1109/TNS.2024.3357129.

[14] L. Yates et al., "Demonstration of >6.0-kV breakdown voltage in large area vertical GaN p-n diodes with step-etched junction termination extensions," *IEEE Trans. Electron Devices*, vol. 69, no. 4, pp. 1931-1937, Apr 2022, doi: 10.1109/TED.2022.3154665.

[15] J. A. Borsuk and R. M. Swanson, "Current transient spectroscopy: A high-sensitivity DLTS system," *IEEE Transactions on Electron Devices*, vol. 27, no. 12, pp. 2217-2225, Dec. 1980, doi: 10.1109/T-ED.1980.20255

[16] D. V. Lang, "Deep-level transient spectroscopy: A new method to characterize traps in semiconductors," *J. Appl. Phys.*, vol. 45, no. 7, pp. 3023-3032, Jul 1974, doi: 10.1063/1.1663719.

[17] J. M. Lauenstein, M. C. Casey, R. L. Ladbury, H. S. Kim, A. M. Phan, and A. D. Topper, "Space radiation effects on SiC power device reliability," *IEEE Int. Rel. Phys. Sym.*, pp. 498-505, Mar 2021, doi: 10.1109/IRPS46558.2021.9405180.

[18] M. A. Ebrish et al., "Impact of anode thickness on breakdown mechanisms in vertical GaN PiN diodes with planar edge termination," *Crystals*, vol. 12, no. 5, Apr 2022, Art. no. 623, doi: 10.3390/cryst12050623.

[19] M. A. Ebrish et al., "Study of anode doping and avalanche in foundry compatible 1.2 kV vertical GaN PiN diodes," *Appl. Phys. Expr.*, vol. 16, no. 11, Nov 2023, Art. no. 116501, doi: 10.35848/1882-0786/ad0655.

[20] A. S. Senarath et al., “Heavy ion-induced single-event leakage current and burnout in homojunction GaN pin diodes,” *IEEE Trans. Nucl. Sci.*, vol. 72, no. 8, pp. 2377-2385, Apr 2025, doi: 10.1109/TNS.2025.3556730.

[21] A. S. Senarath et al., “Single-event burnout in homojunction GaN vertical PiN diodes with hybrid edge temination design,” *Appl. Phys. Lett.*, vol. 124, no. 13, Mar 2024, Art. no. 132101, doi: 10.1063/5.0189744.

[22] N. F. Mott, “Conduction in non-crystalline materials,” *Philos. Mag*., vol. 19, no. 160, pp. 835–852, Dec. 1968, doi: 10.1088/0031-9112/39/8/024.

[23] D. C. Look et al., “Deep-center hopping conduction in GaN,” *J. Appl. Phys*., vol. 80, no. 5, pp. 2960–2963, Sep. 1996, doi: 10.1063/1.363128.

[24] D. Yu, C. Wang, B. L. Wehrenberg, and P. Guyot-Sionnest, “Variable range hopping conduction in semiconductor nanocrystal solids,” *Phys. Rev. Lett.*, vol. 92, no. 21, May 2004, Art. no 216802, doi: 10.1103/PhysRevLett.92.216802.

[25] X. Li et al., “Threshold voltage hysteresis and gate leakage in AlGaN/GaN HEMTs,” *IEEE Trans. Nucl. Sci.*, vol. 72, no. 8, pp. 2357-2367, Aug. 2025, doi: 10.1109/TNS.2025.3551268.

[26] X. Li et al., “Defect and impurity-center activation and passivation in irradiated AlGaN/GaN HEMTs,” *IEEE Trans. Nucl. Sci.*, vol. 71, no. 1, pp. 80-87, Jan. 2024, doi: 10.1109/TNS.2023.3336836.

[27] M. Silvestri, M. J. Uren, and M. Kuball, “Iron-induced deep-level acceptor center in GaN/AlGaN high electron mobility transistors: Energy level and cross section,” *Appl. Phys. Lett*., vol. 102, no. 7, Feb. 2013, Art. no. 073501, doi: 10.1063/1.4793196.

[28] Y. Puzyrev et al., “Gate bias dependence of defect-mediated hot-carrier degradation in GaN HEMTs,” *IEEE Trans. Electron Devices*, vol. 61, no. 5, pp. 1316-1320, May 2014, doi: 10.1109/TED.2014.2309278.

[29] Y. S. Puzyrev, R. D. Schrimpf, D. M. Fleetwood, and S. T. Pantelides, “Role of Fe impurity complexes in the degradation of GaN/AlGaN high-electron-mobility transistors,” *Appl. Phys. Lett.*, vol. 106, no. 5, Feb 2015, Art. no. 053505, doi: 10.1063/1.4907675.

[30] D. Wickramaratne, J.-X. Shen, C. E. Dreyer, A. Alkauskas, and C. G. Van de Walle, “Electrical and optical properties of iron in GaN, AlN, and InN,” *Phys. Rev. B, Condens. Matter*, vol. 99, no. 20, May 2019, Art. no. 205202, doi: 10.1103/PhysRevB.99.205202.

[31] D. M. Fleetwood, X. Li, E. X. Zhang, R. D. Schrimpf, and S. T. Pantelides, “Low-frequency noise due to iron impurity centers in GaN-based HEMTs,” *IEEE Trans. Electron Devices*, vol. 71, no. 2, Feb 2024, doi: 10.1109/TED.2023.3347212.

[32] Y. Zhang et al., “Probing unintentional Fe impurity incorporation in MOCVD homoepitaxy GaN: Toward GaN vertical power devices,” *J. Appl. Phys.*, vol. 127, no. 21, Jun 2020, Art. no. 215707, doi: 10.1063/5.0008758.

[33] C. G. Van de Walle and J. Neugebauer, “First-principles calculations for defects and impurities: Applications to III-nitrides,” *J. Appl. Phys*., vol. 95, no. 8, pp. 3851–3879, Apr. 2004, doi: 10.1063/1.1682673.

[34] T. Roy et al., “Temperature-dependence and microscopic origin of low frequency 1/f noise in GaN/AlGaN high electron mobility transistors,” *Appl. Phys. Lett*., vol. 99, no. 20, Nov. 2011, Art. no. 203501, doi: 10.1063/1.3662041.

[35] Y. S. Puzyrev et al., “Dehydrogenation of defects and hot-electron degradation in GaN high-electron-mobility transistors,” *J. Appl. Phys*., vol. 109, no. 3, Feb. 2011, Art. no. 034501, doi: 10.1063/1.3524185.

[36] R. Jiang et al., “Multiple defects cause degradation after high field stress in AlGaN/GaN HEMTs,” *IEEE Trans. Device Mater. Rel*., vol. 18, no. 3, pp. 364–376, Sep. 2018, doi: 10.1109/TDMR.2018.2847338.

[37] Y. S. Puzyrev, T. Roy, E. X. Zhang, D. M. Fleetwood, R. D. Schrimpf, and S. T. Pantelides, “Radiation-induced defect evolution and electrical degradation of AlGaN/GaN high-electron-mobility transistors,” *IEEE Trans. Nucl. Sci*., vol. 58, no. 6, pp. 2918–2924, Dec. 2011, doi: 10.1109/TNS.2011.2170433.

[38] A. S. Hauck, M. Jin, and B. R. Tuttle, “Nonradiative carrier capture by point defects in irradiated GaN,” *J. Appl. Phys.*, vol. 139, no. 24, Jun 2026, Art. no. 245702, doi: 10.1063/5.0325688.

[39] S. Limpijumnong and C. G. Van de Walle, “Diffusivity of native defects in GaN,” *Phys. Rev. B*, vol. 69, no. 3, Jan. 2004, Art. no. 035207, doi: 10.1103/PhysRevB.69.035207.